

Measurement of Charm Meson Lifetimes

G. Bonvicini,¹ D. Cinabro,¹ R. Greene,¹ L. P. Perera,¹ G. J. Zhou,¹ S. Chan,² G. Eigen,² E. Lipeles,² M. Schmidtler,² A. Shapiro,² W. M. Sun,² J. Urheim,² A. J. Weinstein,² F. Würthwein,² D. E. Jaffe,³ G. Masek,³ H. P. Paar,³ E. M. Potter,³ S. Prell,³ V. Sharma,³ D. M. Asner,⁴ A. Eppich,⁴ J. Gronberg,⁴ T. S. Hill,⁴ C. M. Korte,⁴ D. J. Lange,⁴ R. J. Morrison,⁴ H. N. Nelson,⁴ T. K. Nelson,⁴ D. Roberts,⁴ H. Tajima,⁴ B. H. Behrens,⁵ W. T. Ford,⁵ A. Gritsan,⁵ H. Krieg,⁵ J. Roy,⁵ J. G. Smith,⁵ J. P. Alexander,⁶ R. Baker,⁶ C. Bebek,⁶ B. E. Berger,⁶ K. Berkelman,⁶ V. Boisvert,⁶ D. G. Cassel,⁶ D. S. Crowcroft,⁶ M. Dickson,⁶ S. von Dombrowski,⁶ P. S. Drell,⁶ D. J. Dumas,^{6,*} K. M. Ecklund,⁶ R. Ehrlich,⁶ A. D. Foland,⁶ P. Gaidarev,⁶ L. Gibbons,⁶ B. Gittelman,⁶ S. W. Gray,⁶ D. L. Hartill,⁶ B. K. Heltsley,⁶ S. Henderson,⁶ P. I. Hopman,⁶ N. Katayama,⁶ D. L. Kreinick,⁶ T. Lee,⁶ Y. Liu,⁶ T. O. Meyer,⁶ N. B. Mistry,⁶ C. R. Ng,⁶ E. Nordberg,⁶ M. Ogg,^{6,†} J. R. Patterson,⁶ D. Peterson,⁶ D. Riley,⁶ A. Soffer,⁶ J. G. Thayer,⁶ P. G. Thies,⁶ B. Valant-Spaight,⁶ A. Warburton,⁶ C. Ward,⁶ M. Athanas,⁷ P. Avery,⁷ C. D. Jones,⁷ M. Lohner,⁷ C. Prescott,⁷ A. I. Rubiera,⁷ J. Yelton,⁷ J. Zheng,⁷ G. Brandenburg,⁸ R. A. Briere,⁸ A. Ershov,⁸ Y. S. Gao,⁸ D. Y.-J. Kim,⁸ R. Wilson,⁸ T. E. Browder,⁹ Y. Li,⁹ J. L. Rodriguez,⁹ H. Yamamoto,⁹ T. Bergfeld,¹⁰ B. I. Eisenstein,¹⁰ J. Ernst,¹⁰ G. E. Gladding,¹⁰ G. D. Gollin,¹⁰ R. M. Hans,¹⁰ E. Johnson,¹⁰ I. Karliner,¹⁰ M. A. Marsh,¹⁰ M. Palmer,¹⁰ C. Plager,¹⁰ C. Sedlack,¹⁰ M. Selen,¹⁰ J. J. Thaler,¹⁰ J. Williams,¹⁰ K. W. Edwards,¹¹ A. Bellerive,¹² R. Janicek,¹² P. M. Patel,¹² A. J. Sadoff,¹³ R. Ammar,¹⁴ P. Baringer,¹⁴ A. Bean,¹⁴ D. Besson,¹⁴ D. Coppage,¹⁴ R. Davis,¹⁴ S. Kotov,¹⁴ I. Kravchenko,¹⁴ N. Kwak,¹⁴ L. Zhou,¹⁴ S. Anderson,¹⁵ Y. Kubota,¹⁵ S. J. Lee,¹⁵ R. Mahapatra,¹⁵ J. J. O'Neill,¹⁵ R. Poling,¹⁵ T. Riehle,¹⁵ A. Smith,¹⁵ M. S. Alam,¹⁶ S. B. Athar,¹⁶ Z. Ling,¹⁶ A. H. Mahmood,¹⁶ S. Timm,¹⁶ F. Wappler,¹⁶ A. Anastassov,¹⁷ J. E. Duboscq,¹⁷ K. K. Gan,¹⁷ C. Gwon,¹⁷ T. Hart,¹⁷ K. Honscheid,¹⁷ H. Kagan,¹⁷ R. Kass,¹⁷ J. Lee,¹⁷ J. Lorenc,¹⁷ H. Schwarthoff,¹⁷ A. Wolf,¹⁷ M. M. Zoeller,¹⁷ S. J. Richichi,¹⁸ H. Severini,¹⁸ P. Skubic,¹⁸ A. Undrus,¹⁸ M. Bishai,¹⁹ S. Chen,¹⁹ J. Fast,¹⁹ J. W. Hinson,¹⁹ N. Menon,¹⁹ D. H. Miller,¹⁹ E. I. Shibata,¹⁹ I. P. J. Shipsey,¹⁹ S. Glenn,²⁰ Y. Kwon,^{20,‡} A. L. Lyon,²⁰ E. H. Thorndike,²⁰ C. P. Jessop,²¹ K. Lingel,²¹ H. Marsiske,²¹ M. L. Perl,²¹ V. Savinov,²¹ D. Ugolini,²¹ X. Zhou,²¹ T. E. Coan,²² V. Fadeyev,²² I. Korolkov,²² Y. Maravin,²² I. Narsky,²² R. Stroynowski,²² J. Ye,²² T. Wlodek,²² M. Artuso,²³ S. Ayad,²³ E. Dambasuren,²³ S. Kopp,²³ G. Majumder,²³ G. C. Moneti,²³ R. Mountain,²³ S. Schuh,²³ T. Skwarnicki,²³ S. Stone,²³ A. Titov,²³ G. Viehhauser,²³ J. C. Wang,²³ S. E. Csorna,²⁴ K. W. McLean,²⁴ S. Marka,²⁴ Z. Xu,²⁴ R. Godang,²⁵ K. Kinoshita,^{25,§} I. C. Lai,²⁵ P. Pomianowski,²⁵ and S. Schrenk²⁵

(CLEO Collaboration)

¹Wayne State University, Detroit, Michigan 48202

²California Institute of Technology, Pasadena, California 91125

³University of California, San Diego, La Jolla, California 92093

⁴University of California, Santa Barbara, California 93106

⁵University of Colorado, Boulder, Colorado 80309-0390

⁶Cornell University, Ithaca, New York 14853

⁷University of Florida, Gainesville, Florida 32611

⁸Harvard University, Cambridge, Massachusetts 02138

⁹University of Hawaii at Manoa, Honolulu, Hawaii 96822

¹⁰University of Illinois, Urbana-Champaign, Illinois 61801

¹¹Carleton University, Ottawa, Ontario, Canada K1S 5B6

and the Institute of Particle Physics, Canada

¹²McGill University, Montréal, Quebec, Canada H3A 2T8

and the Institute of Particle Physics, Canada

¹³Ithaca College, Ithaca, New York 14850

¹⁴University of Kansas, Lawrence, Kansas 66045

¹⁵University of Minnesota, Minneapolis, Minnesota 55455

¹⁶State University of New York at Albany, Albany, New York 12222

¹⁷The Ohio State University, Columbus, Ohio 43210

¹⁸University of Oklahoma, Norman, Oklahoma 73019

¹⁹Purdue University, West Lafayette, Indiana 47907

²⁰University of Rochester, Rochester, New York 14627

²¹Stanford Linear Accelerator Center, Stanford University, Stanford, California 94309

²²Southern Methodist University, Dallas, Texas 75275

²³Syracuse University, Syracuse, New York 13244

²⁴Vanderbilt University, Nashville, Tennessee 37235

²⁵Virginia Polytechnic Institute and State University, Blacksburg, Virginia 24061

(Received 8 February 1999)

We report measurements of the D^0 , D^+ , and D_s^+ meson lifetimes using 3.7 fb^{-1} of e^+e^- annihilation data collected near the $\Upsilon(4S)$ resonance with the CLEO detector. The measured lifetimes of the D^0 , D^+ , and D_s^+ mesons are $408.5 \pm 4.1_{-3.4}^{+3.5}$ fs, $1033.6 \pm 22.1_{-12.7}^{+9.9}$ fs, and $486.3 \pm 15.0_{-5.1}^{+4.9}$ fs. The precisions of these lifetimes are comparable to those of the best previous measurements, and the systematic errors are very different. In a single experiment we find that the ratio of the D_s^+ and D^0 lifetimes is 1.19 ± 0.04 . [S0031-9007(99)09313-8]

PACS numbers: 14.40.Lb, 13.25.Ft

The systematics of charm hadron lifetimes have played a central role in understanding heavy quark decays [1]. In this Letter we report new measurements of the lifetimes of the D^0 , D^+ , and D_s^+ mesons. These charm meson ground states differ in the identity of the light antiquark; i.e., the D^0 , D^+ , and D_s^+ mesons are $c\bar{u}$, $c\bar{d}$, and $c\bar{s}$ states. Although the weak decay of the charm quark is responsible for the decays of all three charm mesons, differences in the lifetimes indicate that the identity of the light antiquark also influences the rates of decay. The large ratio [2] of the D^+ and D^0 lifetimes ($\tau_{D^+}/\tau_{D^0} \sim 2.5$) arises primarily from destructive interference between different quark diagrams that contributes significantly only to D^+ decay [1]. This interference and a number of smaller effects, which can cause the D_s^+ and D^0 lifetimes to differ, appear in a systematic expansion, in inverse powers of the charm quark mass, of the QCD contributions to the charm decay amplitudes [1]. The results described in this Letter indicate that the ratio of the D_s^+ and D^0 lifetimes differs significantly from one, providing a quantitative challenge for the theory of charm meson decays. These data were obtained in an e^+e^- colliding beam environment, where the event topologies and backgrounds are very different from those encountered in the high energy fixed target experiments [3] that have recently provided the most precise measurements of D meson lifetimes [2].

The results described in this Letter are based on an integrated luminosity of 3.7 fb^{-1} of e^+e^- annihilation data recorded with the CLEO II.V detector near the $\Upsilon(4S)$ resonance at the Cornell Electron Storage Ring (CESR). The CLEO II detector has been described elsewhere [4]. The major component of the CLEO II.V upgrade is the SVX, the first multilayer silicon vertex detector operating near the $\Upsilon(4S)$ energy [5]. The SVX consists of three concentric layers of $300 \mu\text{m}$ thick, double-sided silicon strip detectors to measure the xy and rz coordinates [6] of charged particles. The three layers are at radii of 2.35, 3.25, and 4.75 cm. There is a total of 0.016 radiation lengths in the material in the SVX and the beryllium beam pipe whose inner radius is 1.875 cm. The average “signal-to-noise” ratio for charged particles at minimum ionization is 15:1 for the xy view and 10:1 for the rz view, and the efficiency to have two or more SVX hits simultaneously in both views is 95% per track. The impact parameter resolutions as functions of momentum p (GeV/ c) are measured from data to be $\sigma_{xy} = 19 \oplus 39/(p \sin^{3/2}\theta) \mu\text{m}$ and (at $\theta = 90^\circ$) $\sigma_{rz} = 50 \oplus 45/p \mu\text{m}$ [7]. The Monte Carlo simulation (MC) of the CLEO detector response is

based upon GEANT [8]. Simulated events are processed in a similar manner as the data.

We reconstruct D mesons in the decay modes $D^0 \rightarrow K^-\pi^+$, $K^-\pi^+\pi^0$, $K^-\pi^+\pi^-\pi^+$, $D^+ \rightarrow K^-\pi^+\pi^+$, and $D_s^+ \rightarrow \phi\pi^+$ with $\phi \rightarrow K^+K^-$. In this Letter, “ D ” refers to D^0 , D^+ , and D_s^+ mesons and reference to the charge conjugate state is implicit. The charged D daughters are required to have well reconstructed tracks and to have particle identification information from specific ionization (dE/dx) and time of flight consistent with the D daughter hypothesis. Charged tracks forming a D candidate are required to originate from a common vertex. Neutral pions are reconstructed from photon pairs detected in the electromagnetic calorimeter. The photons are required to have an energy of at least 30 (50) MeV in the barrel (end cap) region and their invariant mass is required to be within 3 standard deviations of the nominal π^0 mass. The π^0 momentum for $D^0 \rightarrow K^-\pi^+\pi^0$ is required to be greater than 100 MeV/ c . For background suppression, a soft pion π_s^+ (π_s^0) is required to form a D^{*+} with the D candidate for the D^0 (D^+) decay modes. The reconstructed $D^{*+} - D^0$ (D^+) mass difference is required to be within 800 (1400) keV/ c^2 of the nominal value [2]. For the decay $D_s^+ \rightarrow \phi\pi^+$, followed by $\phi \rightarrow K^+K^-$, the K^+K^- invariant mass is required to be within 6 MeV/ c^2 of the ϕ mass, and the helicity angle of the K^+K^- system θ_{KK}^* is required to satisfy $|\cos\theta_{KK}^*| > 0.4$. The D^{*+} and the D_s^+ momenta are required to be greater than 2.5 GeV/ c . The distributions of $M(D)$, the reconstructed invariant mass of the D candidates, are shown in Fig. 1 (after subtracting the nominal D mass values M_D [2]). The numbers of reconstructed D mesons N_D , given in Fig. 1, result from fits to two Gaussians over a linear background. The background fractions in the mass regions within ± 16 MeV of the nominal D mass values [2] are 1.2% ($K^-\pi^+$), 4.9% ($K^-\pi^+\pi^0$), 10.0% ($K^-\pi^+\pi^-\pi^+$), 12.2% (D^+), and 13.8% (D_s^+).

The dimensions of the CESR luminous region (beam spot) are known from the machine optics to be about 1 cm along the beam direction (z), $7 \mu\text{m}$ in the y direction, and about $350 \mu\text{m}$ in the x direction. The centroid of the beam spot is determined [9] for each CESR fill. The D mesons are produced approximately back to back at the interaction point (IP). In the laboratory frame the selected D^0 , D^+ , and D_s^+ mesons have an average momentum of 3.2 GeV/ c and average decay lengths of 200, 500, and 240 μm . The decay vertex \mathbf{r}_D and the momentum vector \mathbf{p}_D of each D meson candidate are reconstructed in the

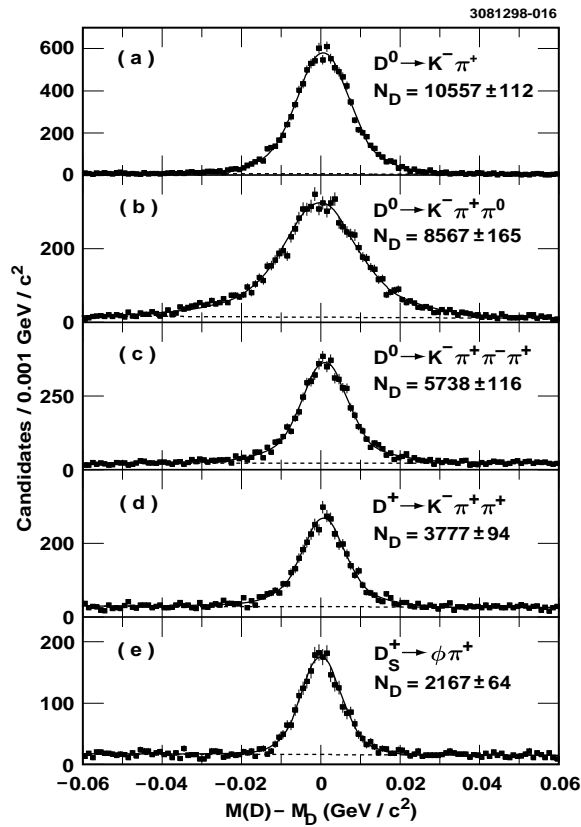


FIG. 1. Masses of charmed meson candidates $M(D)$ minus the nominal masses M_D for (a) $D^0 \rightarrow K^- \pi^+$, (b) $D^0 \rightarrow K^- \pi^+ \pi^0$, (c) $D^0 \rightarrow K^- \pi^+ \pi^- \pi^+$, (d) $D^+ \rightarrow K^- \pi^+ \pi^+$, and (e) $D_s^+ \rightarrow \phi \pi^+$. The data (solid squares) are overlaid with the fit to two Gaussians with the same mean over a linear background (solid line). The fitted background is indicated by the dashed line.

xy plane. The decay vertex resolution along the D flight direction is $80\text{--}100 \mu\text{m}$ depending on the decay mode. The interaction point \mathbf{r}_{IP} is reconstructed by extrapolating the D momentum back from the decay vertex to the beam spot. We calculate the projected decay length l_{dec} from the distance in the xy plane between the IP and the D decay

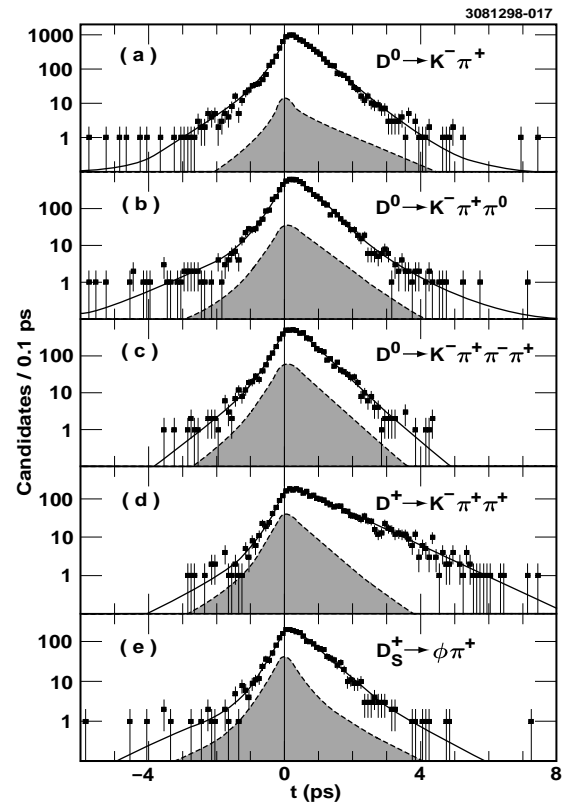


FIG. 2. Proper-time distributions of D meson candidates within $\pm 16 \text{ MeV}/c^2$ of the nominal D mass for (a) $D^0 \rightarrow K^- \pi^+$, (b) $D^0 \rightarrow K^- \pi^+ \pi^0$, (c) $D^0 \rightarrow K^- \pi^+ \pi^- \pi^+$, (d) $D^+ \rightarrow K^- \pi^+ \pi^+$, and (e) $D_s^+ \rightarrow \phi \pi^+$. The data (solid squares) are overlaid with the result from the ULF (solid line). The proper-time spectra of the background candidates obtained from the fits are indicated by the shaded area.

vertex, $l_{\text{dec}} = (\mathbf{r}_D - \mathbf{r}_{\text{IP}}) \cdot \hat{\mathbf{p}}_D$. We then calculate the proper time of the D meson decay from $t = M_D l_{\text{dec}} / c p_D$ using the PDG [2] averages for M_D . The proper-time distributions for the D candidates are shown in Fig. 2.

The D meson lifetimes are extracted from the proper-time distributions with an unbinned likelihood fit (ULF). The likelihood function is

$$L(\tau_D, f_{\text{bg}}, \tau_{\text{bg}}, S, f_{\text{mis}}, \sigma_{\text{mis}}, f_{\text{wide}}) = \prod_i \int_0^\infty dt' \left[\underbrace{p_{\text{sig},i} E(t' | \tau_D)}_{\text{signal fraction}} + \underbrace{(1 - p_{\text{sig},i}) [f_{\text{bg}} E(t' | \tau_{\text{bg}}) + (1 - f_{\text{bg}}) \delta(t')]}_{\text{background fraction}} \right] \\ \times \left[\underbrace{(1 - f_{\text{mis}} - f_{\text{wide}}) G(t_i - t' | S \sigma_{t,i})}_{\text{proper-time resolution}} + \underbrace{f_{\text{mis}} G(t_i - t' | \sigma_{\text{mis}}) + f_{\text{wide}} G(t_i - t' | \sigma_{\text{wide}})}_{\text{mismeasured fraction}} \right],$$

where the product is over the D meson candidates, $G(t | \sigma) \equiv \exp(-t^2/2\sigma^2)/\sqrt{2\pi}\sigma$, and $E(t | \tau) \equiv \exp(-t/\tau)/\tau$. We fit the proper-time distributions for the different decay modes separately. In these fits, each D meson candidate is assigned a signal probability $p_{\text{sig},i}$

based on its mass. The signal probabilities are derived from the (independent) fits of the D mass distributions to the sum of two Gaussians with the same mean and a linear background function. The seven parameters of the lifetime are τ_D , f_{bg} , τ_{bg} , S , f_{mis} , σ_{mis} , and f_{wide} . The

parameter τ_D is the D meson lifetime. The background proper-time distribution is modeled by a fraction f_{bg} with a background lifetime τ_{bg} and a fraction with zero lifetime. In order to estimate the background properties, we fit the candidates in a wide region of ± 40 MeV/ c^2 around the nominal D mass. Each candidate is weighted in the fit according to its proper-time uncertainty $\sigma_{t,i}$. The fit allows for a global scale factor S that modifies the calculated proper-time uncertainty. The fits yield $S \sim 1.1$ for all modes. For a small fraction of mismeasured candidates f_{mis} , the fitted uncertainty $S\sigma_{t,i}$ underestimates the true uncertainty. This results from track reconstruction errors such as hard scattering or the use of an SVX noise hit in the track fit. In the fit, we account for the mismeasured candidates with two Gaussians. The fit parameters associated with the mismeasured candidates are the fraction of events in each of the Gaussians f_{mis} and f_{wide} and the width of one of the Gaussians σ_{mis} . The width of the other Gaussian ($\sigma_{\text{wide}} = 8$ ps) is fixed. The results of the ULFs are superimposed on the proper-time distributions in Fig. 2.

From the fits we obtain $\tau_{D^0} = 411.1 \pm 5.7$ fs ($K^- \pi^+$), 395.2 ± 8.1 fs ($K^- \pi^+ \pi^0$), 416.3 ± 8.6 fs ($K^- \pi^+ \pi^- \pi^+$), $\tau_{D^+} = 1033.6 \pm 22.1$ fs, and $\tau_{D_s^+} = 486.3 \pm 15.0$ fs, where the uncertainties are statistical only. The correlation coefficients between the D lifetime and the other fit parameters are typically near 0.1 and the largest is 0.28. All of these fit results have been corrected for small biases observed in the measurements of the D lifetimes in simulated events of -3.0 ± 0.9 fs ($K^- \pi^+$), 2.4 ± 2.3 fs ($K^- \pi^+ \pi^0$), -2.0 ± 2.2 fs ($K^- \pi^+ \pi^- \pi^+$), -2.9 ± 6.6 fs (D^+), and -0.6 ± 2.4 fs (D_s^+). The D^0 lifetime $\tau_{D^0} = 408.5 \pm 4.1$ fs is the weighted average of the three measurements using statistical uncertainties and the weights $(\tau/\sigma_\tau)^2$ [10].

The large samples of reconstructed charm mesons permit a number of consistency checks, including varying the D candidate mass region, measurement of the background properties in the D mass sidebands, and division of the

data samples in several key variables such as azimuthal angle, polar angle, momentum of the D candidate, and data taking period. No statistically significant effect is found in any of these variables. The systematic uncertainties for the D meson lifetimes are listed in Table I. They can be grouped into three categories:

Reconstruction of the D decay length and proper time.—Errors in the measurement of the reconstructed decay length can be due to errors in the measurement of the decay vertex, the global detector scale, and the beam spot. The bias in the decay vertex position is estimated to be 0.0 ± 0.9 μm from a “zero-lifetime” sample of $\gamma\gamma \rightarrow \pi^+ \pi^- \pi^+ \pi^-$ events. This corresponds to a measured proper-time uncertainty of ± 1.8 fs. In addition, the vertex reconstruction is checked with events with interactions in the beam pipe with a relative uncertainty of $\pm 0.2\%$. The global detector scale is measured to a precision of $\pm 0.1\%$ in surveys. The sums of these uncertainties in quadrature yield the systematic uncertainties due to the decay vertex measurement. The changes in the lifetimes due to the variation (± 2 μm) in the vertical beam spot position and height are another source of systematic error, since they are used in the calculation of the IP. Statistical uncertainties for the D masses [2] and the D momentum measurements lead to systematic errors since these quantities are used to convert the decay length into proper time.

Lifetime fit procedure.—This category includes uncertainties in the candidate signal probabilities, the impact of candidates with large proper times, the correlation between proper time and D meson mass, and the proper-time properties of the background. The signal probability assigned to each candidate in the lifetime fit has a statistical uncertainty, and these statistical uncertainties lead to systematic uncertainties in the fitted lifetimes. We estimate these systematic uncertainties by coherently varying the signal probability of each candidate by its statistical uncertainty and repeating the fits. A correlation between the measurements of the proper time t and the D candidate mass $M(D)$ can be a source of systematic

TABLE I. Systematic uncertainties for the D meson lifetimes in fs. The systematic uncertainties for the three D^0 modes are weighted with the same weights as the fitted D^0 lifetimes.

Uncertainty	D^0			D^0 Combined	D^+ $K^- \pi^+ \pi^+$	D_s^+ $\phi \pi^+$
	$K^- \pi^+$	$K^- \pi^+ \pi^0$	$K^- \pi^+ \pi^- \pi^+$			
Decay vertex	± 2.0	± 2.0	± 2.0	± 2.0	± 2.8	± 2.1
Global detector scale	± 0.1	± 0.1	± 0.1	± 0.1	± 0.1	± 0.1
Beam spot	+0.3 -0.1	+2.1 -0.0	+0.3 -0.2	+0.8 -0.1	+1.3 -1.1	+0.7 -1.1
D meson mass	± 0.1	± 0.1	± 0.1	± 0.1	± 0.3	± 0.1
D meson momentum	+0.2 -0.0	+0.1 -0.2	+0.3 -0.1	+0.2 -0.1	+0.6 -0.0	± 0.1
Signal probability	+0.4 -0.1	+0.1 -0.2	+0.1 -0.2	+0.3 -0.1	+1.2 -0.8	+1.3 -1.8
$t - M(D)$ correlation	± 0.6	± 0.6	± 1.0	± 0.7	± 1.7	± 1.5
Large proper times	± 1.2	± 3.4	± 0.2	± 1.5	± 0.3	± 0.5
Background	± 0.5	± 2.4	± 3.0	± 1.5	± 6.3	± 2.9
MC statistics	± 0.9	± 2.3	± 2.2	± 1.6	± 6.6	± 2.4
Total	+2.7 -2.6	+5.6 -5.2	± 4.4	+3.5 -3.4	+9.9 -12.7	+4.9 -5.1

uncertainty. We measure this correlation in simulated events to estimate the associated systematic uncertainty. Charm meson candidates with large proper times are an additional source of systematic uncertainty. These candidates are modeled by the wide Gaussian in the proper-time fit. Alternatively, the wide Gaussian component is omitted from the likelihood function and candidates in a restricted proper-time interval are fitted. The systematic uncertainties due to candidates with large proper times are estimated from the variations of τ_D with the width of the wide Gaussian and the differences in the results between the fits with different proper-time intervals. This systematic uncertainty is small for decay modes with three or more charged D daughters for which the requirement of a well-reconstructed vertex greatly reduces mismeasurements. We estimate the systematic uncertainty due to backgrounds that might populate the D mass peaks differently than they populate the D mass sidebands, $20 \text{ MeV}/c^2 < |M(D) - M_D| < 60 \text{ MeV}/c^2$. Some possible sources of such backgrounds are a background in the D_s^+ sample from $D^+ \rightarrow K^+ \pi^- \pi^-$ decays where one π^- is misidentified as a K^- , and backgrounds from $D^{+(0)}$ decays in the $D^{0(+)}$ sample caused by adding or missing a charged pion.

Checking the algorithms with simulated events.—Candidate selection requirements can cause systematic biases in the lifetime measurements. We estimate these biases with simulated events and correct for the biases as described above. We include the statistical uncertainties in the measured lifetimes from the samples of simulated events as systematic uncertainties in the results.

The total systematic uncertainties in the D^0 lifetime measurement are obtained by combining the contributions from the three reconstructed D^0 decay modes. The contributions from the decay length measurement and the detector size are assumed to be completely correlated and all other contributions are assumed to be uncorrelated. The total systematic uncertainties are obtained by adding the individual contributions in quadrature.

In summary, our measured D lifetimes are $\tau_{D^0} = 408.5 \pm 4.1_{-3.4}^{+3.5}$ fs, $\tau_{D^+} = 1033.6 \pm 22.1_{-12.7}^{+9.9}$ fs, and $\tau_{D_s^+} = 486.3 \pm 15.0_{-5.1}^{+4.9}$ fs, where the first uncertainties are statistical and the second systematic. These results imply $\tau_{D_s^+}/\tau_{D^0} = 1.19 \pm 0.04$, a difference of more than 4.5 standard deviations in a single experiment. The charm meson lifetimes reported in this Letter are

comparable in precision with the best previous measurements [3], and the systematic errors are very different.

We gratefully acknowledge the effort of the CESR staff in providing us with excellent luminosity and running conditions. We wish to acknowledge and thank the technical staff, who contributed to the success of the CLEO II.V detector upgrade, including J. Cherwinka and J. Dobbins (Cornell); M. O'Neill (CRPP); M. Haney (Illinois); M. Studer and B. Wells (OSU); K. Arndt, D. Hale, and S. Kyre (UCSB). We appreciate contributions from G. Lutz and advice from A. Schwarz. This work was supported by the National Science Foundation, the U.S. Department of Energy, Research Corporation, the Natural Sciences and Engineering Research Council of Canada, the A.P. Sloan Foundation, the Swiss National Science Foundation, and the Alexander von Humboldt Stiftung.

*Permanent address: Computing Devices Canada, Nepean, ON, Canada K2H 5B7.

†Permanent address: University of Texas, Austin, Texas 78712.

‡Permanent address: Yonsei University, Seoul 120-749, Korea.

§Permanent address: University of Cincinnati, Cincinnati, OH 45221.

- [1] G. Bellini, I. Bigi, and P.J. Dornan, Phys. Rep. **289**, 1 (1997).
- [2] Particle Data Group, C. Caso *et al.*, Eur. Phys. J. C **3**, 1 (1998).
- [3] E687 Collaboration, P.L. Frabetti *et al.*, Phys. Rev. Lett. **71**, 827 (1993); E687 Collaboration, P.L. Frabetti *et al.*, Phys. Lett. B **323**, 459 (1994); E791 Collaboration, E.M. Aitala *et al.*, Phys. Lett. B **445**, 449 (1999).
- [4] CLEO Collaboration, Y. Kubota *et al.*, Nucl. Instrum. Methods Phys. Res., Sect. A **320**, 66 (1992).
- [5] T. Hill, Nucl. Instrum. Methods Phys. Res., Sect. A **418**, 32 (1998).
- [6] The right-handed coordinate system has the z axis along the e^+ beam direction and the y axis upward.
- [7] Later improvement of the track-fitting code results in an rz impact parameter resolution of $\sigma_{rz} = 42 \oplus 45/p \mu\text{m}$ at $\theta = 90^\circ$.
- [8] R. Brun *et al.*, GEANT 3.15, CERN Report No. DD/EE/84-1 (1987).
- [9] D. Cinabro *et al.*, Phys. Rev. E **57**, 1193 (1998).
- [10] L. Lyons and D.H. Saxon, Rep. Prog. Phys. **52**, 1015 (1989).